Journal of Materials Chemistry A

ROYAL SOCIETY OF CHEMISTRY

COMMUNICATION

View Article Online
View Journal | View Issue

Cite this: J. Mater. Chem. A, 2023, 11, 1651

Received 17th October 2022
Accepted 12th December 2022

DOI: 10.1039/d2ta08102d

rsc.li/materials-a

Super-efficient fire safety poly(lactide) enabled by unique radical trapping†

Dan Xiao, *[a] Song Chen,[a] Fang-Juan Wu,[a] Zhi-Yu Xiao,[b] Zi-Bo Wang[a] and Hui Fang[a]

Poly(lactic acid) (PLA) as a promising bio-plastic will decompose to small molecule flammable volatiles *via* chain scission, which thus exhibit poor fire safety and highly restrict its real-world applications. Herein, we report a novel multifunctional furan bio-based fire retardant (F-FR). The comprehensive properties of the F-FR in PLA were investigated systematically. As a result, the multifunctional F-FR exhibited not only good thermal stability, high crystallization behavior and excellent transparency, but also super-efficient fire safety regarding self-extinguishing. It was interesting that only trace 0.8 wt% loading of F-FR in PLA was needed to attain the UL-94 V-0 grade. For the first time, the LOI result of PLA with 2 wt% F-FR was as high as 48.0%. More importantly, the unique furan radical trapping mechanism from theoretical and experimental results in the gas phase was simulated and proved by quantum chemical calculations and the compositions and structures of molecules from the degradation and pyrolysis of F-FR, oxygen and PLA radicals. This work offers a useful and green strategy for developing super-efficient eco-friendly additives, enriches the fire-safety mechanism of PLA, and has promising broad application in engineering materials.

With the depletion of fossil resources and deterioration of the environment, petroleum-based plastic and pollution has become an urgent environmental issue all over the world.[1,2] Degradable polymers from nature, as one of the most promising sustainable plastics, should be developed.[3,4] Poly(lactic acid) (PLA), as a promising bio-plastic can be biodegraded to generate water (H_2O) and carbon dioxide (CO_2), and has become one of the most widely used biodegradable materials due to its excellent biodegradability, good appearance and high tensile property. Nevertheless, PLA decomposes to small molecule flammable volatiles *via* chain scission, which thus exhibit poor fire safety and highly restrict its real-world applications because of the high potential fire risk.

To fit the required fire safety standards, extensive studies have been conducted on the pyrolysis and combustion behavior of PLA.[5–7] As shown in Fig. 1, generally speaking, the pyrolysis of small molecules and free radicals (oxygen (O˙), hydrogen (H˙) and hydroxyl (OH˙)) of PLA can be firstly generated after heating. Apart from that, these free radicals and heat can decompose the matrix as well as support flammable small molecule reactions.[8,9] Currently, the addition of fire-retardants (FR) is the most important economically in the fire safety field. For example, the FR radicals (*e.g.* chlorine (Cl˙) and bromine (Br˙) radicals) can be produced by pyrolysis of halogenated flame retardants (H-FR), which trap the supporting radicals generated from burning (*e.g.* OH˙ and H˙) to interrupt the combustion reaction in the gas-phase. Nevertheless, nowadays, some H-FR are gradually being prohibited due to environmental issues.

Recently, sustainable biological FR additives, such as lignin,[10–14] cellulose,[15–17] starch,[18,19] chitosan (CS),[20–23] protein,[24] β-cyclodextrin (CD),[25,26] polydopamine (PDA),[29] phytic acid (PA),[30–33] vegetable oils, furan (FA)[35–37] *etc.* have become a hot and attractive topic.[2–6] In general, the fire safety mechanism of bio-based FRs can be divided into the condensed-phase and the gas-phase.

On the one hand, in the condensed-phase, some bio-based FRs have been adopted due to their outstanding residue formation. For instance, Zhang *et al.*[10] reported that the LOI

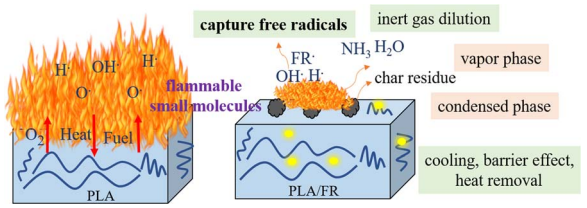

Fig. 1 Illustration of the fire-retardant mechanism for PLA.

[a]Key Laboratory of Polymer Materials and Products of Universities in Fujian, Department of Materials Science and Engineering, Fujian University of Technology, Fuzhou, Fujian, 350108, China. E-mail: 19872102@fjut.edu.cn

[b]School of Materials Science and Engineering, Guilin University of Electronic Technology, Guilin, 541004, China

† Electronic supplementary information (ESI) available. See DOI: https://doi.org/10.1039/d2ta08102d

result of PLA containing 19% ammonium polyphosphate (APP) and 4% urea modified lignin reached 34.5% and the UL-94 V-0 grade was attained. According to Maqsood *et al.*,[11] the LOI result of PLA with 3% kraft lignin and 20% APP reached 36.6% and the UL-94 V-0 grade was achieved. As pointed out by Tawiah *et al.*,[12] the LOI result of PLA following addition of 15 wt% calcium sulfonated lignin additives reached 28.8% and the UL-94 V-0 grade was achieved. As claimed by Zhu *et al.*,[15] the LOI with 3% modified cellulose and 7% APP reached 26.8% and the UL-94 V-0 grade was achieved. Moreover, the LOI result of PLA containing 10% modification with FR cellulose nanofiber reached 25.8% and the UL-94 V-0 grade was achieved.[16] At the same time, He *et al.*[17] reported that the LOI result of PLA with 10 wt% phosphazene-containing cellulose nanocrystals and APP reached 28.1% and the UL-94 V-0 grade was obtained. Wang *et al.*[18] investigated the LOI result of PLA with 30% APP and starch which was found to reach 41.0% and the UL-94 V-0 grade was achieved. Maqsood *et al.*[19] reported that the LOI of PLA with 27 wt% starch and APP reached 37.3% and the UL-94 V-0 grade was achieved. As stated by Xiong *et al.*,[20] adding 10 wt% core–shell structure of a bio-based FR met the UL-94 V-0 grade. Beyond that, Zhang *et al.*[21] explored the LOI result of PLA with 10 wt% fire-retardant, which reached 30.6% and met the UL-94 V-0 grade. As demonstrated by Chen *et al.*,[22] the LOI result of PLA with 7 wt% CS and APP reached 33% and the UL-94 V-0 grade was reached. Zhang *et al.*[24] mentioned that the LOI result of PLA/20% casein compounds reached 32.2% with a UL-94 V-0 rating. As pointed out by Feng *et al.*,[25] the LOI result of PLA containing 20 wt% FR (weight ratio of CD/APP/MA (melamine) was 1 : 2 : 1) reached 34.2% with UL-94 V-0 grading. Besides, Decsov *et al.*[26] claimed that the LOI result of PLA with 15 wt% modified FR CD reached 37.5% with UL-94 V-0 grading. According to Jing *et al.*,[27] the LOI of PLA with 10% APP–BPE (BPE)–PEI (PEI) reached 27.5% with a UL-94 V-0 rating and that of PLA with a core–shell structure of 10% APP–BPE–PEI reached 27.5% with a UL-94 V-0 rating.[28] Zhang *et al.*[29] reported that the LOI result of PLA/15 wt% PDA flax fiber compounds reached 26.1% with a UL-94 V-2 rating. When PLA with a bio-based FR is burned, charred layer structures are formed to inhibit transformation of the combustible small molecules, heat and oxygen.[2,45,46] Unfortunately, the required high loading (more than 10%) based on the condensed phase FR may destroy the mechanical properties of polymeric materials.

On the other hand, to improve fire safety efficiency, other bio-based intermediates based on the gas-phase have been designed due to the generation of FR free radicals. For example, Zhou *et al.*[30] reported that the LOI of PLA with 3 wt% modified PA was enhanced to 30.5% and the UL-94 V-0 grade was achieved. Also Ye *et al.*[31] reported that PLA with 2 wt% PF (PA and FA) passed the V-0 grade, and PLA with 4 wt% PF exhibited a LOI of 28.5%. By synthesizing a bio-based furan FR, Sun *et al.*[34] found that PLA with 2 wt% bio-based furan FR had a LOI of 29.6% and the UL-94 V-0 grade was reached. Moreover, Xiao *et al.*[35] synthesized the bio-based phenyl *P*-(*N*–*N*′-di-(furan-2-ylmethyl)) phosphonamidate (PFPA). The LOI result of PLA with 3 wt% of PFPA reached 30.7% and passed the V-0 grade in a UL-94 test. Xiao *et al.*[36] synthesized the bio-based *N*-(furan-2-ylmethyl)-*P*,*P*-diphenylphosphinic amide (FPPA), and the LOI result of PLA with 3 wt% of FPPA reached 33.8% and passed the V-0 grade. Therefore, the LOI and UL-94 results of PLA with different types and loadings of bio-based FRs are demonstrated in Fig. 2. However, there are still some areas that need to be improved. First of all, compared with H-FRs, bio-based FRs are still not efficient. Secondly, the bio-based raw materials based on gas-phase FRs are more effective than the condensed phase FRs for PLA in terms of LOI and UL-94. More importantly, the detailed gas-phase fire safety mechanism needs to be further clarified.

Very recently, bio-based phenylphosphonic difurfurylamine (PPDF) was synthesized.[37] The LOI result of PLA with 0.8 wt% PPDF reached 30.0% and the V-0 grade was passed.[37] To obtain super-efficient bio-based FR materials and to understand the fire safety mechanism more deeply, herein, we report a novel multifunctional furan bio-based fire retardant (F-FR). The comprehensive properties of F-FR in PLA were investigated systematically. As a result, the multifunctional F-FR exhibited not only good thermal stability, high crystallization behavior and excellent transparency, but also super-efficient fire safety regarding self-extinguishing. The fire safety mechanism from theoretical and experimental results in the gas phase was simulated and proved. This work may be expanded to other bio-

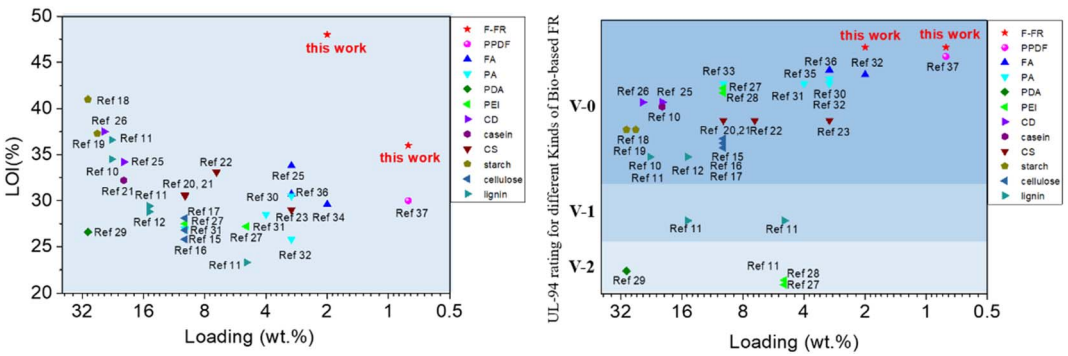

Fig. 2 LOI and UL-94 rating of different bio-based flame retardant PLAs as a function of loading.

polymer systems to develop high-performance fire-safety polymers.

The preparation of F-FR is displayed in Fig. 1S–4S.† According to the FTIR results, the P=O bond (1187 cm^{-1}), aromatic rings (1631, 1469 and 1436 cm^{-1}), P–N–C (1056 and 729 cm^{-1}) and N–H (3240 and 3172 cm^{-1}) bonds are characteristic peaks of F-FR. As exhibited in Fig. 3S,† the peaks corresponding to the hydrogens in the benzene ring (7.85 ppm and 7.45 to 7.23 ppm), the methylene and secondary amine (4.92 to 4.78 ppm) and the protons in the tetrahydrofuran ring (1.52 to 1.92 ppm) are characteristic peaks of F-FR. As shown by the mass spectrum, the experimental value of F-FR is 326.9 g mol^{-1} (theoretical value M + $2H^+$: 326.1) in Fig. 4S.† Thus, F-FR was synthesized successfully according to the FTIR, NMR, and MS results.

The detailed thermal behavior including the 5 wt% mass loss temperature (T_{onset}), maximum weight loss rate (R_{max}), maximum weight loss temperature (T_{max}) and char residue is displayed in Fig. 5S and Table 1S.† The T_{onset} of F-FR was 205 °C. From Fig. 5S,† the R_{max1} and T_{max1} values of F-FR are 1.1%/°C and 313 °C respectively. The T_{max2} and R_{max2} results of F-FR were 442 °C and 0.44%/°C, respectively. Beyond that, the char residues of F-FR amounted to 17.1% (500 °C) and 16.2% (600 °C). The T_{onset} values of PLA with 0.5%, 0.8%, and 2% F-FR contents under a nitrogen atmosphere were 331, 328 and 322 °C, respectively. Apart from that, the R_{max} values of PLA with 0.5%, 0.8% and 2% F-FR under a nitrogen atmosphere were 4.8, 3.9 and 2.8%/°C, respectively. The T_{onset} values of PLA with 0.5%, 0.8%, and 2% F-FR contents in air were 335, 332 and 327 °C, respectively. Moreover, the R_{max} values of PLA with 0.5%, 0.8% and 2% F-FR in air were 3.5, 2.7 and 2.2%/°C, respectively. These results indicated that the R_{max} values were lower in air than under a nitrogen atmosphere. Moreover, addition of a F-FR in PLA could result in high thermal properties.

UL-94, a conventional method in industry, was used to evaluate the flammability of the polymers.[5–8,38,39] From Fig. 3a and 6S,† it is apparent that PLA, an extremely flammable polymer, can be ignited quickly, with fire droplets also igniting the cotton. However, with the loading of F-FR, the flammability of the PLA composites reduced obviously in the UL-94 test. When 0.5 wt% F-FR was added, the PLA composites achieved a V-1 rating in the UL-94 test. Surprisingly, PLA containing 0.8 wt% and 2 wt% F-FR achieved the UL-94 V-0 grade. It was known that the droplets of PLA were serious during PLA burning. With the addition of F-FR, the number of droplets of the PLA/F-FR composites gradually reduced. Moreover, the droplets of the PLA/F-FR composites cannot ignite cotton due to the superior self-extinguishing of F-FR in the gas-phase. Therefore, only trace loading of the F-FR in PLA displayed super-efficient fire safety regarding self-extinguishing.

The LOI as the minimum amount of O_2 to support the burning of materials was also used to test the flammability of

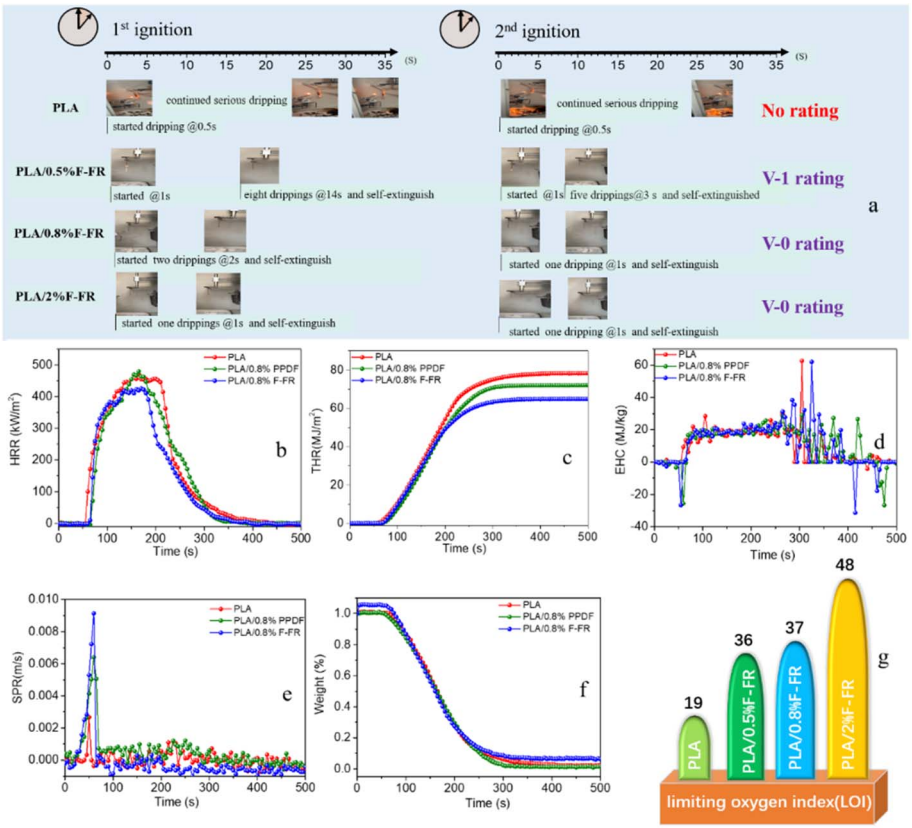

Fig. 3 Combustion behavior of F-FR. (a) Real-time photos at different times in the UL-94 test, (b) heat release rate (HRR), (c) total heat release (THR), (d) effective heat combustion (EHC), (e) smoke release rate (SPR), (f) mass loss (ML) and (g) LOI results of PLA and PLA/F-FR composites.

PLA in industry. The LOI of neat PLA was 19%, which is below the normal atmospheric oxygen concentration (21%). Surprisingly, with a loading of 0.5 and 0.8 wt% F-FR, the LOI of PLA/0.5% F-FR and PLA/0.8% F-FR composites was as high as 36 and 37% respectively. Generally speaking, the oxygen index of a refractory material is more than 27%. For the first time, the LOI result of PLA containing 2 wt% F-FR was as high as 48.0% in Fig. 3g. Thus, F-FR resulted in super-efficient fire safety of PLA.

In order to better investigate the combustion behavior of F-FR, the cone-calorimeter results of the pure PLA, PLA/PPDF and PLA/F-FR composites are shown in Fig. 3b–f. Obviously, the maximum heat release rate results of the pure PLA and PLA with 0.8 wt% PPDF composites were 479 and 472 kW m^{-2}. The maximum heat release rate of the PLA/0.8% F-FR composite was 425 kW m^{-2}. Thus, F-FR was more efficient than PPDF in the fire safety of PLA. Beyond that, the ignition time of the PLA, PLA/0.8% PPDF and PLA/0.8% F-FR composites was 55, 65, and 65 s respectively. The ignition time result of PLA/F-FR was 10 s greater than that of PLA, which means more escape time in a fire. Besides, the maximum total heat release of pure PLA and PLA with 0.8 wt% PPDF content was 78 MJ m^{-2} and 72 MJ m^{-2} respectively. According to Fig. 3c, the THR of PLA/0.8% F-FR was reduced to 64 MJ m^{-2}. The effective heat combustion value and mass loss result are shown in Fig. 3d and f. The effective heat combustion (EHC) of PLA with 0.8 wt% F-FR content was delayed, indicating outstanding fire safety in the gas-phase. The smoke production rate (SPR) result of the PLA, PLA/PPDF and PLA/F-FR composites is displayed in Fig. 3e. The SPR of PLA was 0.0023 m^2 s^{-1}. Beyond that, the SPR result of PLA with 0.8 wt% F-FR content increased to 0.0091 m^2 s^{-1} because the combustion of the PLA/F-FR composites in the gas-phase was restricted.[5–9,40,41] Since the F-FR could not catalyze the charring of PLA, the incorporation of F-FR did not increase the charring of PLA. Thus, at the end of burning, the cone-calorimeter test showed limited carbon residue of PLA with 0.8% F-FR (Fig. 3f).

To investigate in-depth the super-efficient fire safety action, the condensed and gas-phase components and products were considered systematically. Thin char residues of PLA (Fig. 7S(a)†) and PLA/0.8% F-FR composites (Fig. 7S(b)†) were generated after the combustion. The SEM images of the inner surface (c) and outer surface (d) residues of PLA/0.8% F-FR composites were fluffy, thin, and discontinuous. Moreover, there was no obvious graphitization characteristic peak in the Raman spectrum in Fig. 8S.† According to the analysis of char residue, the condensed-phase action of fire safety is not the main reason.

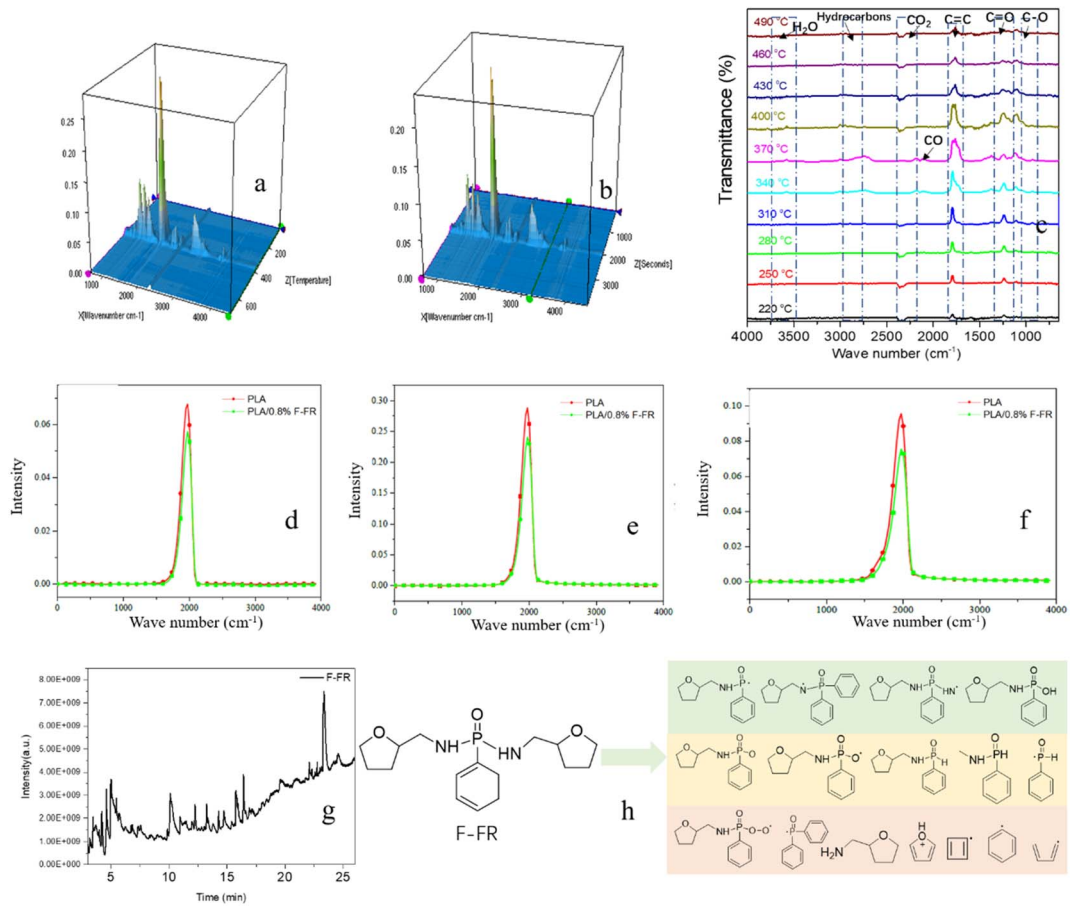

Fig. 4 The components and products in the gas-phase. 3D FTIR degradation products of PLA (a) and PLA/0.8% F-FR composites (b) at different temperatures; TG-FTIR results of degradation products of PLA/0.8% F-FR composites (c) at different temperatures; intensity *vs.* wave number curves of hydrocarbons (d), aldehydes (e), and carbonyl compounds (f); Py-GC-MS result of F-FR (g), the pyrolysis products of F-FR (h).

The components and products in the gas-phase during PLA/F-FR composite combustion are displayed in Fig. 4. Relative to PLA (Fig. 4(a)), the main gaseous components of PLA with 0.8 wt% F-FR are similar in Fig. 4(b). The main degradation components of PLA with 0.8 wt% F-FR were carbonyl compounds (~1748 cm^{-1}), carbon monoxide (2168–2121 cm^{-1}), aldehydes (2761–2687 cm^{-1}), H_2O (3618–3537 cm^{-1}), carbon dioxide (2632–2379 cm^{-1}), hydrocarbons (3023–2865 cm^{-1}) and other components, as displayed in Fig. 4(c). According to degradation components in the vapor phase of PLA/0.8 wt% F-FR composites at 325 °C in Fig. 4(c), the absorption peaks at 1621, 1587, 1562, 1431, 1240, 1053, 924 and 907 cm^{-1} might be associated with the presence of FR radicals and ammonia, which inhibited and diluted the release of flammable small molecules during degradation of the PLA matrix in the gas-phase. Moreover, from Fig. 4(d–f), the intensity *vs.* wave number results of the hydrocarbons, aldehydes, and carbonyl compounds of PLA/0.8 wt% F-FR composites were clearly reduced relative to PLA because of the inhibition effect of F-FR in the gas-phase. The major pyrolysis products of F-FR from Py-GC/MS at 500 °C in Fig. 4g and Table 2S† were FR radicals and their derivatives, which conformed with the results of TG-FTIR. Moreover, the addition of F-FR changed the degradation pathway of PLA, and FR radicals (*e.g.* phosphorus, benzene, phosphooxygen and phosphooxygen dibenzene, *etc.*) were formed by pyrolysis of the F-FR in Fig. 4h. Overall, these specific radicals could stabilize or trap radicals for supporting PLA combustion in the gas-phase.

According to combustion products and components from Py-GC-MS and TG-FTIR, the possible reaction between PLA and the F-FR under oxygen is shown in Fig. 10S and 11S.† What's more, the degradation or pyrolysis products are simulated using Material Studio software in Fig. 12S.† In this simulation, the radical trapping mechanisms of the LUMO (Lowest Unoccupied Molecular Orbital) and HOMO (Highest Occupied Molecular Orbital) were simulated by $Dmol^3$ included in the Material Studio software. Hence, the binding energies of the degradation or pyrolysis products are simulated in Table 1. Traditionally speaking, the phosphorus-containing flame retardants (P-FR) can form phosphorus radicals which stabilize or trap supporting radicals produced from burning (*e.g.* H•, OH•) to interrupt PLA combustion in the gas phase.[4–9,41,42] However, as displayed in Table 1 and Fig. 5, the binding energies of radicals of F-FR with a hydroxyl radical (OH•), hydrogen radical (H•) and oxygen (O_2), (adsorption of oxygen near PLA) were 113.3, 105.9 and 31.7 kcal mol^{-1}, respectively. Apart from that, the binding energies of radicals of F-FR with oxygen O (oxygen atom) and an oxygen free radical O• (conjugate structure with oxygen) were 132.5 and 179.4 kcal mol^{-1}, respectively. Obviously, F-FR with oxygen (O) or an oxygen free radical (O•) is much more stable. Moreover, the binding energies of radicals of F-FR with different PLA radicals were 124, 14.2 and 98.6 kcal mol^{-1}, respectively. Thus, the main reasons for super-efficient fire safety of F-FR are as follows. During the burning of the PLA matrix, free radicals and small molecules can be produced *via* chain scission and elimination reactions. Prior to the ignition of the polymer, F-FR is firstly decomposed to produce FR free radicals. Furthermore, these unique radical trapping free radicals capture free oxygen or oxygen radicals. The reaction was stopped due to a lack of oxygen between the fire-retardant and polymer. When the polymer was ignited, FR radicals (*e.g.* phosphorus, benzene, phosphooxygen, phosphooxygen benzene, *etc.*) were formed by thermal degradation of F-FR. Indeed, these radicals could not only stabilize or trap radicals for supporting PLA combustion, but could also stop the burning *via* a chain reaction in the gas-phase.

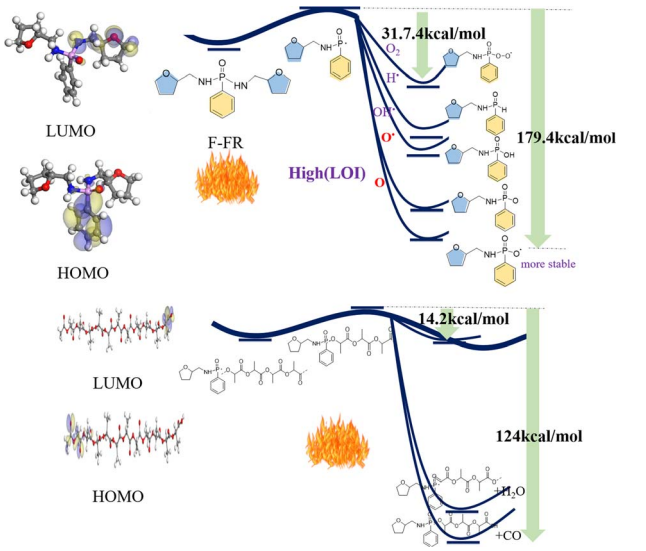

Fig. 5 Simulated degradation and combustion behavior. The binding energies of the degradation and combustion behavior were obtained by using the Material Studio software. The radical trapping mechanisms of the LUMO (Lowest Unoccupied Molecular Orbital) and HOMO (Highest Occupied Molecular Orbital) were simulated by quantum chemistry ($Dmol^3$ included in Material Studio software).

Table 1 Binding energy of degradation or pyrolysis products are simulated by Material Studio software

Free radicals	Binding energy of pyrolysis PPDF (kcal mol^{-1})	Binding energy of pyrolysis F-FR (kcal mol^{-1})
OH•	115.1	113.3
H•	105.7	105.9
O_2	83.3	31.7
O•	132.3	132.5
O	179.4	179.7
PLA1	20.6	124.0
PLA2	14.1	14.2
PLA3	92.9	98.6

The non-isothermal crystallization melting behaviors are displayed in Fig. 13S and Table 3S.† The X_c of PLA with 0.5%, 0.8%, and 0.2% F-FR contents was 6.4, 10.35, 11.17 and 12.72%, respectively. Obviously, with the addition of F-FR, the crystallization rate and crystallinity of PLA were enhanced. Compared with the T_m (melting temperature) and T_{cc} (cold crystallization peak temperature) of pure PLA (170 and 107 °C), the T_m and T_{cc} of PLA with F-FR loading were smaller and lower since F-FR

promoted the formation of crystals of PLA, and improved the crystallization rate and crystallinity of PLA.

Isothermal crystallization values of pure PLA and PLA/F-FR composites are displayed in Fig. 14S and Table 4S.† Meanwhile, isothermal crystallization results of $\ln[-\ln(1 - X_t)]$ *vs.* $\ln(t)$ of PLA and PLA/F-FR at 100 °C (a), 105 °C (b), 110 °C (c) and 115 °C (d) are presented in Fig. 14S.† In Table 4S,† n equals ~2–3 with the addition of F-FR, revealing that F-FR is an effective nucleating agent which improved the heterogeneous nucleation significantly. In addition, as shown in Table 4S,† the $t_{1/2}$ (half time of PLA crystallization) of the PLA/F-FR composites was distinctly lower compared with that of PLA, indicating that F-FR effectively improved the crystal formation, crystallization rate, and heterogeneous nucleation of PLA/F-FR composites.

To deeply understand the crystallization behaviors, the POM (polarizing optical microscope) results at 115 °C are displayed in Fig. 15S.† When PLA was heated to 200 °C, then cooled to 115 °C, there was almost no crystal formation. After 5 minutes, crystals of PLA were gradually produced. With the introduction of F-FR, the size and number of crystals of PLA significantly increased as time went on. Moreover, the contour of PLA/F-FR composites was not clear due to the number of crystals increasing. Based on non-isothermal crystallization, isothermal crystallization and crystallization behavior results, the multifunctional F-FR exhibits not only super-efficient fire-retardancy, but is also a highly-efficient nucleating agent.

The tensile and transparency results are shown in Table 5S and Fig. 16S.† The tensile result of PLA was ~65.4 MPa. With introduction of 0.5 wt% F-FR, the tensile result of PLA was 65.2 MPa. The tensile strength of PLA with 0.8 wt% F-FR and 2 wt% F-FR was 61.3 and 56.3 MPa. Meanwhile, the transparency results of PLA with 0.5 wt% F-FR and 8 wt% F-FR had a nice state (Fig. 18S†). These results indicated that the tensile and transparency properties of PLA with a suitable loading of F-FR did not reduce much. Moreover, the DMA results of the PLA and PLA/F-FR composites are shown in Fig. 17S.† From Fig. 17S(a),† the storage modulus of the PLA and PLA/F-FR composites was basically unchanged from 35 to 50 °C. With the increase of temperature, the storage modulus of the PLA and PLA/F-FR composites rapidly reduced because of the glass transition temperature (T_g) being reached. Relative to neat PLA (998 MPa), the storage modulus of the PLA/0.5% F-FR composites was 970 MPa, which did not reduce much. In Fig. 17S(b),† only one peak appeared in the tan δ *vs.* temperature plot, showing that there was good compatibility between PLA and F-FR. Compared with that of neat PLA (62 °C), the T_g of PLA with F-FR content reduced, which was in agreement with the molten drop in the UL-94 test.[43,44]

In summary, we reported a novel multifunctional furan bio-based fire retardant (F-FR). The comprehensive properties of the F-FR in PLA were investigated systematically. As a result, the multifunctional F-FR exhibited not only good thermal stability, high crystallization behavior and excellent transparency, but also super-efficient fire safety regarding self-extinguishing. It was interesting that only trace 0.8 wt% loading of F-FR in PLA was needed to attain the UL-94 V-0 grade. For the first time, the LOI result of PLA with 2 wt% F-FR was as high as 48.0%. More importantly, the unique furan radical trapping mechanism from theoretical and experimental results in the gas phase was simulated and proved by quantum chemical calculations and the composition and structures of molecules from the degradation and pyrolysis of F-FR, oxygen and PLA radicals. Overall, its high applicability not only makes it a universal fire-safety state-of-the-art method for PLA, but also provides a new strategy and enriches the fire-safety mechanism for biopolymers.

Conflicts of interest

The authors declare no competing financial interest.

Acknowledgements

D. X. acknowledges the financial support from Science Foundation of the Fujian Province (No. 2020J05191), and Starting Research Fund from Fujian University of Technology (No. GY-Z15002, No. GY-Z19047). H. F. acknowledges the support from Central Government Fund for Guiding Local Scientific and Technological Development (2021L3015).

Notes and references

1 R. Geyer, J. R. Jambeck and K. L. Lew, *Sci. Adv.*, 2017, **3**, e1700782.
2 I. Magaña, R. López, F. J. Enríquez-Medrano, S. Kumar, A. Aguilar-Sanchez, R. Handa, R. D. León and L. Valencia, *J. Mater. Chem. A*, 2022, **10**, 5019–5043.
3 T. Mekonnen, P. Mussone, H. Khalil and D. Bressler, *J. Mater. Chem. A*, 2013, **1**, 13379–13398.
4 C. Jehanno, J. W. Alty, M. Roosen, S. D. Meester, A. P. Dove, Y.-X. Chen, F. A. Leibfarth and H. Sardon, *Nature*, 2022, **603**, 803–814.
5 S. Bourbigot and G. Fontaine, *Polym. Chem.*, 2010, **1**, 1413–1422.
6 B. Tawiah, B. Yu and B. Fei, *Polymers*, 2018, **10**, 876.
7 Y. Xue, J. Feng, Z. Ma, L. Liu, Y. Zhang, J. Dai, Z. Xu, S. Bourbigot, H. Wang and P. Song, *Mater. Today Phys.*, 2021, **21**, 100568.
8 X. Wang, E. Kalalia, J. Wan and D.-Y. Wang, *Prog. Polym. Sci.*, 2017, **69**, 22.
9 B.-W. Liu, L. Chen, D.-M. Guo, X.-F. Liu, Y.-F. Lei, X.-M. Ding and Y. Z. Wang, *Angew. Chem., Int. Ed.*, 2019, **58**, 9188–9193.
10 R. Zhang, X. Xiao, Q. Tai, H. Huang and Y. Hu, *Polym. Eng. Sci.*, 2012, 2620–2626.
11 M. Maqsood, F. Langensiepen and G. Seide, *Molecules*, 2019, **24**, 1513.
12 B. Tawiah, B. Yu, W. Yang, R. K. K. Yuen and B. Fei, *Polym. Adv. Technol.*, 2019, **30**, 2207–2220.
13 L. Costes, F. Laoutid, M. Aguedo, A. Richel, S. Brohez, C. Delvosalle and P. Dubois, *Eur. Polym. J.*, 2016, **84**, 652–667.
14 H. Yang, B. Yu, X. Xu, S. Bourbigot, H. Wang and P. Song, *Green Chem.*, 2020, **22**, 2129–2161.
15 T. Zhu, J. Guo, B. Fei, Z. Feng, X. Gu, H. Li, J. Sun and S. Zhang, *Cellulose*, 2020, **27**, 2309–2323.

16 J. Feng, Y. Sun, P. Song, W. Lei, Q. Wu, L. Liu, Y. Yu and H. Wang, *ACS Sustainable Chem. Eng.*, 2017, **5**, 7894–7904.
17 J. He, Z. Sun, Y. Chen, B. Xu, J. Li and L. Qian, *Cellulose*, 2022, **29**, 6143–6160.
18 X. Wang, Y. Hu, L. Song, S. Xuan, W. Xing, Z. Bai and H. Lu, *Ind. Eng. Chem. Res.*, 2011, **50**, 713–720.
19 M. Maqsood and G. Seide, *Polymers*, 2019, **11**, 48.
20 Z. Xiong, Y. Zhang, X. Du, P. Song and Z. Fang, *ACS Sustainable Chem. Eng.*, 2019, **7**, 8954–8963.
21 Y. Zhang, Z. Xiong, H. Ge, L. Ni, T. Zhang, S. Huo, P. Song and Z. Fang, *ACS Sustainable Chem. Eng.*, 2020, **8**, 6402–6412.
22 C. Chen, X. Gu, X. Jin, J. Sun and S. Zhang, *Carbohydr. Polym.*, 2017, **157**, 1586–1593.
23 X. Ma, N. Wu, P. Liu and H. Cui, *Carbohydr. Polym.*, 2022, **287**, 119317.
24 S. Zhang, X. Jin, X. Gu, C. Chen, H. Li, Z. Zhang and J. Sun, *J. Appl. Polym. Sci.*, 2018, **135**, 46599.
25 J.-X. Feng, S.-P. Su and J. Zhu, *Polym. Adv. Technol.*, 2011, **22**, 1115–1122.
26 K. E. Decsov, B. Ötvös, G. Marosi and K. Bocz, *Polym. Degrad. Stab.*, 2022, **200**, 109938.
27 J. Jing, Y. Zhang, X. Tang, Y. Zhou, X. Li, B. K. Kandola and Z. Fang, *Polymer*, 2017, **108**, 361–371.
28 J. Jing, Y. Zhang, Z.-P. Fang and D.-Y. Wang, *Compos. Sci. Technol.*, 2018, **165**, 161–167.
29 L. Zhang, Z. Li, Y.-T. Pan, A. P. Yáñez, S. Hu, X.-Q. Zhang, R. Wang and D.-Y. Wang, *Composites, Part B*, 2018, **154**, 56–63.
30 Y. Zhou, B. Tawiah, N. Noor, Z. Zhang, J. Sun, R. K. K. Yuen and B. Fei, *Composites, Part B*, 2021, **215**, 108833.
31 G. Ye, S. Huo, C. Wang, Q. Shi, Z. Liu and H. Wang, *Polym. Degrad. Stab.*, 2021, **192**, 109696.
32 L. Haurie Ibarra, Y. Yang, D. Wang, J. Zhang, X. Zhang and R. Wang, *eXPRESS Polym. Lett.*, 2020, **14**, 705–716.
33 S. Qiu, Y. Li, P. Qi, D. Meng, J. Sun, H. Li, Z. Cui, X. Gu and S. Zhang, *Int. J. Biol. Macromol.*, 2021, **193**, 44–52.
34 J. Sun, L. Li and J. Li, *Chem. Eng. J.*, 2019, **369**, 150–160.
35 D. Xiao, M.-T. Zheng, F.-J. Wu, X.-X. Cao, X.-F. Huang, L. Huang and X.-Q. Xiao, *Polym. Degrad. Stab.*, 2022, **203**, 110060.
36 D. Xiao, J.-X. Lv, F.-J. Wu, Z.-B. Wang, K. Harre, J.-H. Chen, U. Gohs and D.-Y. Wang, *Int. J. Biol. Macromol.*, 2022, **215**, 646–656.
37 D. Xiao, Z.-B. Wang, U. Gohs, K. Harre and D.-Y. Wang, *Chem. Eng. J.*, 2022, **446**, 137092.
38 B. Yu, Y. Shi, B. Yuan, S. Qiu, W. Xing, W. Hu, L. Song, S. Lo and Y. Hu, *J. Mater. Chem. A*, 2015, **3**, 8034–8044.
39 L. Zhang, Q. Wang, R.-K. Jian and D.-Y. Wang, *J. Mater. Chem. A*, 2020, **8**, 2529–2538.
40 D. Xiao, M.-T. Zheng, U. Gohs, U. Wagenknecht, B. Voit and D.-Y. Wang, *J. Appl. Polym. Sci.*, 2022, **139**, 52311.
41 Z. Xiang, X. Zhu, Y. Dong, X. Zhang, Y. Shi, W. Lu and Y. Hu, *J. Mater. Chem. A*, 2021, **9**, 17538–17552.
42 N. Wang, S. Chen, L. Li, Z. Bai, J. Guo, J. Qin, X. Chen, R. Zhao, K. Zhang and H. Wu, *J. Phys. Chem. C*, 2021, **125**, 5185–5196.
43 Y. Xu, S. Zhang, X. Peng and J. Wang, *Eur. Polym. J.*, 2018, **99**, 250–258.
44 K. Ru, S. Zhang, X. Peng, J. Wang and H. Peng, *Polymer*, 2019, **185**(17), 121967.
45 B. Gao, T. Shi, X. Yang and S. Zhang, *Composites, Part B*, 2022, **246**, 110145.
46 T. Shi, S. Zhang and X. Shi, *Cellulose*, 2021, **28**, 2995–3015.